

# **Probabilistic representation of driver space and its inference from trajectory data**

Yiru Jiao\*<sup>1</sup>, Sander van Cranenburgh<sup>2</sup>, Simeon C. Calvert<sup>1</sup>, and Hans van Lint<sup>1</sup>

<sup>1</sup>Department of Transport & Planning, Delft University of Technology, The Netherlands

<sup>2</sup>Department of Engineering Systems and Services, Delft University of Technology, The Netherlands

## **SHORT SUMMARY**

Driver space describes the vehicle-centred area where other road users cannot intrude without causing discomfort. It is traditionally measured by a deterministic distance to the boundary within which discomfort is caused. However, driver space is better regarded as probabilistic because intrusion into the driver space may cause varying levels of discomfort. In this study, we present a probabilistic representation of driver space, which conceptually captures the proximity resistance of a vehicle to its surrounding vehicle. Specifically, we develop a method to empirically infer driver space and demonstrate the method by applying it to an urban trajectory dataset. Our results show that driver space grows quadratically with the relative speed of a vehicle to its surrounding vehicle. Furthermore, we find that the longitudinal boundaries of driver space are significantly less sharp than the lateral ones. This implies that traditional distance-based approaches are inadequate for the longitudinal measurement of driver space.

**Keywords:** driver space, probabilistic representation, urban vehicle trajectories, personal space measurement.

**Words:** 2992 (including the summary)

## 1. INTRODUCTION

Personal space is widely known as the area surrounding an individual into which others cannot intrude without causing discomfort (Sommer, 1959; Hayduk, 1978). In 1987, Marsh and Collett proposed that drivers extended their personal space beyond the vehicles. Such extended personal space of a driver was then named by Hennessy, Howard, and Carr (2011) as **driver space**. It covers the physical and social surroundings of a vehicle.

Including driver space, personal space has been represented as a portable territory around an individual (vehicle). It is measured by the (dis)comfort distance from the individual. Hennessy et al. (2011) presented the first projection experiment for measuring driver space, which was also used by Hennessy (2015) and Zhang et al. (2019). In the experiment, participants were shown a top-view image where a car is centred in the right lane of a two-lane roadway. Then they were asked to imagine a hypothetical driving situation and to draw a box around the target vehicle. The box was considered as the projected driver space. Other approaches to measuring personal space besides projection can be found in a summary by Leichtmann and Nitsch (2020).

Such distance-based representation and measurement are deterministic, but the utilisation of driver space often needs to be probabilistic. This is because spatial intrusion may cause different levels of discomfort, e.g., due to unobserved factors of the driver situation as well as heterogeneity across drivers. Cheng and Sester (2018) utilised driver space<sup>1</sup> to evaluate collision risk. To convert the deterministic distance into probabilistic risk, they set the collision probability to be 1 inside driver space and to decrease exponentially as extending outwards driver space. However, such conversion has two drawbacks. Firstly, it does not consider that vehicles with different relative speeds can cause different discomfort even in the same position. Secondly, a predefined probability without empirical evidence may underestimate the discomfort or risk caused by intrusion. Driver space immediately surrounds a vehicle, where this underestimation could involve serious hazards.

In this study, we present a probabilistic representation of driver space and propose a method to empirically infer it from trajectory data. The probabilistic representation is based on not only distance but also velocity. Driver space essentially describes the resistance of a driver to the proximity of other road users. Complementary to this, the presence of other road users reflects the proximity tolerance of the driver. We thus propose to represent driver space using a probability function of proximity resistance. Denote the proximity resistance of an ego vehicle  $i$  to another vehicle  $j$  by  $p_j$ , then the proximity tolerance of  $i$  to  $j$  is  $1 - p_j$ . The cumulative product of  $1 - p_j$  then represents the joint probability of the proximity tolerance of  $i$  to its surrounding vehicles. With adequate data of vehicle trajectories, the function  $p$  can be derived by finding a set of parameters that maximise the joint probability.

The probabilistic representation and its inference offer an empirical approach to approximate the driver space of a vehicle in a given scenario. This can facilitate the utilisation of driver space in multiple fields such as conflict analysis, obstacle avoidance, and route planning.

## 2. METHODOLOGY

### *Coordinate transformation*

Global coordinates need to be transformed to local coordinates when considering the proximity resistance between two vehicles. To do so we take the following steps. Firstly, we construct the

---

<sup>1</sup>Although not claimed as driver space, the authors depicted “vehicle geometry” that resembled pedestrians’ personal space, which is essentially driver space.

transformed coordinate system. Say an ego vehicle  $i$  and a surrounding vehicle  $j$  of  $i$ . The driver space of  $i$  is centered at the position of  $i$ ,  $O_i$ . This study argues that driver space is not a constant territory, but varies with the relative velocity of the involved vehicles. So the driver space of  $i$  is considered to stretch along the relative velocity between  $i$  and  $j$ ,  $\mathbf{v}_{ij}$ , instead of the heading direction of  $i$ . Thereby, a local coordinate system  $C(O_i, \mathbf{v}_{ij})$  is constructed with  $O_i$  as the origin and  $\mathbf{v}_{ij}$  as the y-axis direction.

Secondly, we formulate the transformation equation. Letting  $(x^{(g)}, y^{(g)})$  denote the global coordinates of a vehicle's position and  $(x^{(ij)}, y^{(ij)})$  denote the transformed coordinates in  $C(O_i, \mathbf{v}_{ij})$ , the transformation equation is

$$\begin{bmatrix} x^{(ij)} \\ y^{(ij)} \end{bmatrix} = \begin{bmatrix} \cos \rho & -\sin \rho \\ \sin \rho & \cos \rho \end{bmatrix} \left( \begin{bmatrix} x^{(g)} \\ y^{(g)} \end{bmatrix} + \begin{bmatrix} a \\ b \end{bmatrix} \right), \quad (1)$$

where  $\rho$  indicates the counterclockwise rotation angle and  $(a, b)^\top$  indicates the translation vector of the transformation.

Thirdly, we solve the transformation parameters. Denote the global position of  $i$  as  $(x_{O_i}^{(g)}, y_{O_i}^{(g)})$  and the relative velocity between  $i$  and  $j$  as  $(x_{\mathbf{v}_{ij}}^{(g)}, y_{\mathbf{v}_{ij}}^{(g)})$ . We substitute  $(x^{(g)}, y^{(g)}) = (x_{O_i}^{(g)}, y_{O_i}^{(g)})$  and  $(x^{(ij)}, y^{(ij)}) = (0, 0)$  into equation (1), then substitute  $(x^{(g)}, y^{(g)}) = (x_{O_i}^{(g)} + x_{\mathbf{v}_{ij}}^{(g)}, y_{O_i}^{(g)} + y_{\mathbf{v}_{ij}}^{(g)})$  and  $(x^{(ij)}, y^{(ij)}) = (0, \sqrt{x_{\mathbf{v}_{ij}}^{(g)2} + y_{\mathbf{v}_{ij}}^{(g)2}})$  into equation (1). So that the transformation parameters between the global coordinate system and  $C(O_i, \mathbf{v}_{ij})$  are solved as

$$\begin{cases} a = -x_{O_i}^{(g)}, \\ b = -y_{O_i}^{(g)}, \\ \cos \rho = y_{\mathbf{v}_{ij}}^{(g)} / \sqrt{x_{\mathbf{v}_{ij}}^{(g)2} + y_{\mathbf{v}_{ij}}^{(g)2}}, \\ \sin \rho = x_{\mathbf{v}_{ij}}^{(g)} / \sqrt{x_{\mathbf{v}_{ij}}^{(g)2} + y_{\mathbf{v}_{ij}}^{(g)2}}, \end{cases} \quad (2)$$

where  $\mathbf{v}_{ij}$  should have a non-zero mode, i.e.,  $(x_{\mathbf{v}_{ij}}^{(g)}, y_{\mathbf{v}_{ij}}^{(g)}) \neq (0, 0)$ . Under this condition, relatively stationary vehicles are not considered.

The coordinate transformation gives meaning to the origin and y-axis. It compresses the information about the relative position and relative velocity between  $i$  and  $j$  into 3 variables  $x$ ,  $y$ , and  $v$ . Among them,  $(x, y) = (x_{O_j}^{(ij)}, y_{O_j}^{(ij)})$  and holds the information about the position of  $j$  relative to  $i$  and the direction of  $\mathbf{v}_{ij}$ .  $v = \sqrt{x_{\mathbf{v}_{ij}}^{(g)2} + y_{\mathbf{v}_{ij}}^{(g)2}}$  indicates the mode of  $\mathbf{v}_{ij}$ . Therefore, in this study, longitudinal direction indicates the direction along the relative velocity, and lateral direction indicates the direction perpendicular to the relative velocity.

### ***Probabilistic representation of driver space***

After the transformation, the scatter plots of the surrounding vehicle positions would show the intuitive shape of driver space. Figure 1 shows how such scatter plots of surrounding vehicles could look like. In fact, the scatter plots shown here are based on the dataset we will later use in this study (see Section 3). Figure 1(a) presents a series of scatter plots of  $(\mathbf{x}, \mathbf{y})$  between ego vehicles and their surrounding vehicles. In each plot, the ego vehicle is marked by a red circle,

and the surrounding vehicles marked by blue circles are at the same  $v$ <sup>2</sup>. Figure 1(b) zooms in on the scatter plot where  $v$  is around 6 m/s.

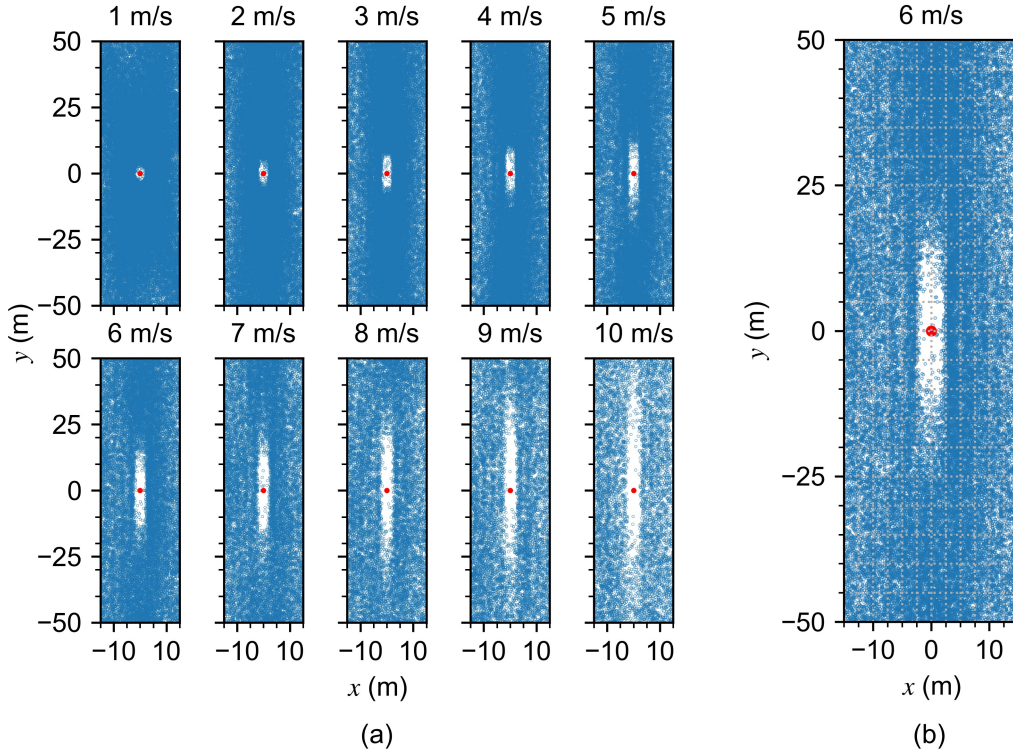


**Figure 1: Scatter plots of surrounding vehicles show driver spaces of ego vehicles. (a) Scatter plots of surrounding vehicles at different  $v$ . (b) The zoomed-in scatter plot of surrounding vehicles at  $v = 6$  m/s.**

Figure 1(a) shows a zone around the ego vehicle where other vehicles are present significantly less often. This zone grows as  $v$  increases. Figure 1(b) shows that the zone is not homogeneous, where there is a sub-zone that vehicles rarely pass through. A transition connects this sub-zone to the normal space outside. Thereby, driver space is a vehicle-centred space where other road users are infrequently present, which covers a private area through which even fewer vehicles pass.

We use proximity resistance to explain the infrequent presence of vehicles in driver space. Proximity resistance is low if another vehicle is sufficiently distant. As another vehicle enters the driver space and approaches the private area of the vehicle, proximity resistance gradually increases. Then when another vehicle enters the private area of the vehicle, proximity resistance peaks.

Based on the above observation and reasoning, we formulate the probabilistic representation of driver space as a probability function of proximity resistance. Given an ego vehicle  $i$ , when the relative position and relative velocity of another vehicle to  $i$  are transformed into  $(x, y, v)$ , the proximity resistance of  $i$  to the vehicle is

<sup>2</sup>Here and in the following experiments,  $v = v_0$  is discretised as  $v$  in the interval of  $(v_0 - 0.1, v_0 + 0.1]$ .

$$p_i(x, y, v | r_x, r_y, \beta_x, \beta_y) = \exp \left( - \left| \frac{x}{r_x} \right|^{\beta_x} - \left| \frac{y}{r_y} \right|^{\beta_y} \right),$$

where

$$\begin{cases} r_x = f_x(v), \\ r_y = f_y(v), \\ \beta_x = \frac{1+\text{sgn}(x)}{2} \beta_x^+ + \frac{1-\text{sgn}(x)}{2} \beta_x^-, & \beta_x^+ \geq 2 \text{ and } \beta_x^- \geq 2, \\ \beta_y = \frac{1+\text{sgn}(y)}{2} \beta_y^+ + \frac{1-\text{sgn}(y)}{2} \beta_y^-, & \beta_y^+ \geq 2 \text{ and } \beta_y^- \geq 2. \end{cases} \quad (3)$$

The shape of formula (3) allows for a plateau and the descent at the boundaries of the plateau.  $r_x$  and  $r_y$  determine the lateral and longitudinal radius of the plateau respectively, and their relations to  $v$  can be investigated by controlling  $v$ . The relations may be different in different traffic scenarios. The  $\beta$ s determine the descent rate at different boundaries of the plateau.  $\beta_x$  is the descent rate at the boundary along  $y$ -axis. If the surrounding vehicles has  $x$  larger than 0,  $\beta_x = \beta_x^+$ , and if  $x$  is smaller than 0,  $\beta_x = \beta_x^-$ .  $\beta_y^+$  and  $\beta_y^-$  are the descent rates at the both boundaries along  $x$ -axis and follow a similar logic. The larger the  $\beta$ s, the faster the discomfort caused by space intrusion near the boundaries increases as a surrounding vehicle approaches the ego vehicle.

### ***Inference of driver space from trajectory data***

We infer driver space by estimating the probability function of proximity resistance from trajectory data. Proximity resistance and proximity tolerance complement one another, where the former is reflected by the absence of other road users and the latter by the presence of other road users. Proximity resistance cannot be directly measured because its reflection is things that do not happen. Therefore, we estimate proximity resistance indirectly by estimating proximity tolerance from the presence of vehicles surrounding an ego vehicle.

The probabilistic driver space of a vehicle  $i$  is given in formula (3) as  $p_i$  the proximity resistance of  $i$ , so the proximity tolerance of  $i$  is  $1 - p_i$ . Considering the likelihood (joint probability) of the presence of  $n$  surrounding vehicles

$$L = \prod_{j=1}^n [1 - p_i(x_j, y_j, v_j)], \quad (4)$$

parameters of  $p_i$  can be estimated by maximising  $L$ . Note that the likelihood for Maximum Likelihood Estimation (MLE) is usually formulated with probability density, whereas the probability of the event is directly used here. This allows for the sparsity of distant vehicles in the data. Distant vehicles outside the driver space are always in probability close to 1. Thereby, MLE can ensure good estimation for the parameters even if vehicles farther away from the ego vehicle are relatively few.

Further practical details need to be considered in the estimation. For convenience, the logarithm of  $L$ , i.e., the sum of the log probability of each surrounding vehicle, is taken as the maximisation objective. Theoretically, surrounding vehicles are not supposed to appear in the private area of an ego vehicle, but in reality some vehicles do. Such vehicles are in extremely small log probability, which makes parameter estimation biased towards overly small  $\beta$ s and  $r$ s. To mitigate this bias,  $\varepsilon = 10^{-4}$  is added to the probability function of proximity tolerance. In this way, the log-likelihood for parameter estimation is

$$\ln(L) = \sum_{j=1}^n \ln[1 + \varepsilon - p_i(x_j, y_j, v_j)]. \quad (5)$$

This study proposes Algorithm 1 to iteratively estimate the parameters of  $p_i$  and thus infer the driver space. It estimates  $\beta$ s given  $r$ s and estimates  $r$ s given  $\beta$ s, where the former is based on maximising  $\ln(L)$  but the latter is not. Holding other parameters constant,  $\ln(L)$  is monotonically decreasing with  $r_x$  or  $r_y$ . Maximising  $\ln(L)$  therefore drives  $r_x$  and  $r_y$  to 0. However,  $r_x$  and  $r_y$  should distinguish the area around the ego vehicle where other vehicles rarely pass. Given constant  $\beta$ s,  $\ln(L)$  goes through three phases with increasing  $r_x$  (or  $r_y$ ). In the first phase,  $\ln(L)$  increases slightly when all vehicle samples are outside the driver space. In the second phase,  $\ln(L)$  decreases slowly when some samples are present in the driver space. In the third phase,  $\ln(L)$  decreases rapidly when more vehicle samples are falsely covered by the driver space. Thus,  $r_x$  and  $r_y$  can be determined by the point at which  $\ln(L)$  decreases from slowly to rapidly. This point is where the second-order derivative of  $\ln(L)$  with respect to  $r_x$  (or  $r_y$ ) is smallest (negative), signalling the fastest change in the decreasing rate of  $\ln(L)$ .

---

**Algorithm 1:** Iterative inference of driver space.

---

**Data:**  $x, y$  given a particular  $v$

**Result:**  $r_x, r_y, \beta_x^+, \beta_x^-, \beta_y^+, \beta_y^-$

**begin**

Initialise  $r_x \leftarrow 1, r_y \leftarrow 1.5, \beta_x^+ \leftarrow 20, \beta_x^- \leftarrow 20, \beta_y^+ \leftarrow 20, \text{ and } \beta_y^- \leftarrow 20$

**repeat**

$r_x \leftarrow \operatorname{argmin} \frac{\partial}{\partial r_x} \left( \frac{\partial \ln(L)}{\partial r_x} \right)$ , subject to  $r_x \geq 1$

$r_y \leftarrow \operatorname{argmin} \frac{\partial}{\partial r_y} \left( \frac{\partial \ln(L)}{\partial r_y} \right)$ , subject to  $r_y \geq 1.5$

$\beta_x^+, \beta_x^-, \beta_y^+, \beta_y^- \leftarrow \operatorname{argmax} \ln(L)$ , subject to  $\beta \geq 2$

**until**  $r_x, r_y, \beta_x^+, \beta_x^-, \beta_y^+, \beta_y^-$  converge **or** max. number of iterations is reached

---

Because the derivative of  $\ln(L)$  to one parameter depends on the other parameters, Algorithm 1 is difficult to solve by hand. Therefore, we take numerical methods to solve the differentiation and optimisation in the algorithm. To narrow the search space, two constraints on  $r_x$  and  $r_y$  are imposed to exclude impossible solutions because the driver space cannot be smaller than a vehicle itself. The parameters are estimated when the iterations converge. The convergence is either to a set of values or several repeated sets of values. In the latter case, the set of values with the largest  $r_y$  is taken, considering that smaller  $r_y$  could increase unnecessary safety risk. In addition, a maximum number of iterations is set to force a stop.

### 3. RESULTS AND DISCUSSION

#### *Dataset and its preprocessing*

We used the pNEUMA dataset (Barmounakis & Geroliminis, 2020) to demonstrate our methodology. With a swarm of 10 drones, pNEUMA records vehicle traces in a congested area of Athens. Video data captured by the drones cover more than 100 km of road network and around 100 busy intersections. Processed by vision algorithms, pNEUMA produces the position, speed, and acceleration of all vehicles at 25 frames per second.

To prepare suitable data for this study, we did 3 steps of preprocessing. First, excluding pedestrians, bicycles, and motorcycles as they have very different movement characteristics regarding

speed and occupied space. Second, removing vehicles that overlap ( $< 0.5$  m) another vehicle's trajectory as it is impossible. This error could be caused by the vision algorithm used to track the trajectories. Third, sampling and transforming coordinates. In this study, cars and taxis that appear for more than 30s are considered as ego vehicles. For each deemed as an ego vehicle, a number of moments 30s apart are selected according to their appearing duration. At the selected moments, the transformation coordinate system is constructed between the ego vehicle and each other vehicle appearing simultaneously. Finally, in the transformed coordinate system, surrounding vehicles that are at a distance of 100m from the ego vehicle along  $x$ -axis or  $y$ -axis are recorded as samples.

In this way, personal preferences for driver space are acceptably ignored. Because the influence on driver space caused by personal preference, in this study, is considered to be much less than that caused by vehicle size and relative velocity between vehicles.

### ***Inferred driver space under different relative speeds***

We obtained more than 15 million pairs of samples. Using 0.2 m/s as the interval of relative speed, in total 65 times of estimation of the probabilistic representation were performed from 0 m/s to 13 m/s. In each estimation,  $x$  and  $y$  are verified to be independent with correlation coefficients ranging from  $-0.0285$  to  $0.0063$ .

Taking the situations when  $v = 1$  m/s to  $v = 7$  m/s as examples, Figure 2 is a visual comparison of the inference results with the real-world data. Figure 2(a) shows the scatter plots of the positions of the surrounding vehicles. Figure 2(b) plots the logarithmic frequencies of the surrounding vehicles in  $0.5 \times 0.5$  m<sup>2</sup> grids. Figure 2(c) then shows the heat maps of the inferred driver space. The comparison shows that our method to infer probabilistic driver space accurately fits the data. In addition, it intuitively shows that the transitions at the longitudinal boundaries of driver space are longer than that at the lateral ones.

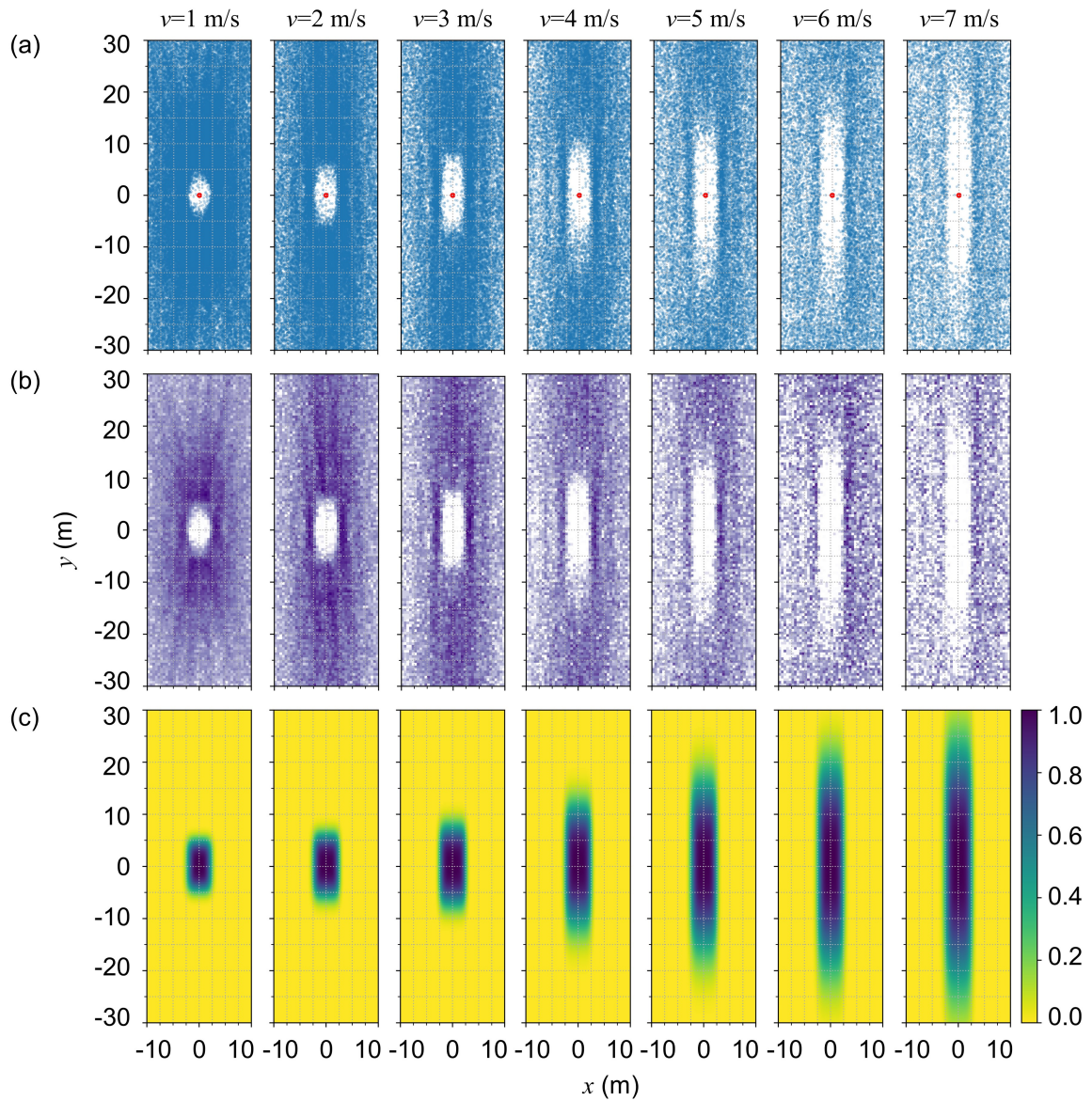
### ***Driver space as a function of relative position and relative speed***

With this series of estimation under different relative speeds, we formulated the averaged driver space of cars and taxis in pNEUMA dataset. It is a probability function of relative position ( $x, y$ ) and relative speed  $v$  according to formula (3), where  $f_x(v)$  and  $f_y(v)$  are fitted to the estimates.

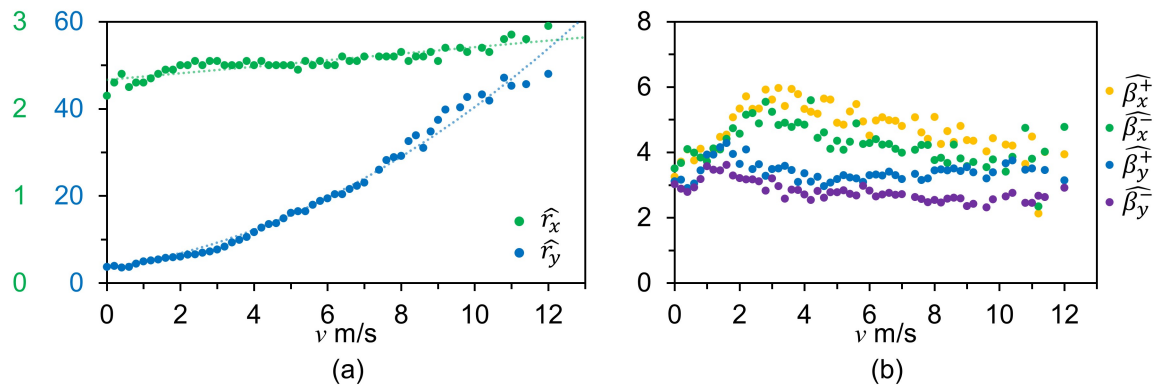
The estimates of  $r_x$ ,  $r_y$ ,  $\beta_x^+$ ,  $\beta_x^-$ ,  $\beta_y^+$ , and  $\beta_y^-$  are evaluated together by two criteria. First, the estimates are rejected if at least one of them degenerates to the lower bounds they are subjected to. Second, the estimation of  $\beta$ s by maximising  $\ln(L)$  offers the calculation of  $p$  values, so the estimates are rejected when at least one of the  $p$  values is larger than 0.05. Figure 3 plots the accepted estimates<sup>3</sup>.

Figure 3(a) shows that  $\hat{r}_x$  and  $\hat{r}_y$  grow as  $v$  is larger, and  $\beta$ s are increasingly stable with larger  $v$ . The increase relations of  $\hat{r}_x$  and  $\hat{r}_y$  with  $v$ , i.e.,  $f_x(v)$  and  $f_y(v)$ , are best fitted as a linear and a quadratic formula, respectively. Setting the intercept with the estimate at  $v = 0$ , 0.78 of the variation in  $\hat{r}_x$  is explained by  $\hat{r}_x = 0.0623v + 2.15$ , and 0.99 of the variation in  $\hat{r}_y$  is explained by  $\hat{r}_y = 0.2526v^2 + 1.1650v + 3.55$ . The averages of  $\hat{\beta}_x^+$ ,  $\hat{\beta}_x^-$ ,  $\hat{\beta}_y^+$ , and  $\hat{\beta}_y^-$  are around 4.776, 4.298, 3.413, and 2.815, respectively. Taking them together, function (6) is obtained as the averaged driver space,

<sup>3</sup>The estimates at  $v = 11.2$  m/s, i.e.,  $\hat{r}_x = 2.35$ ,  $\hat{r}_y = 50.30$ ,  $\hat{\beta}_x^+ \approx 2.132$ ,  $\hat{\beta}_x^- \approx 2.348$ ,  $\hat{\beta}_y^+ \approx 625.011$ ,  $\hat{\beta}_y^- \approx 2.672$ , are excluded in the following statistics. Because the  $\hat{\beta}_y^+$  is too large and is considered as an outlier.



**Figure 2: Comparison between real-world data and the inference results. (a) Positions of surrounding vehicles. (b) Logarithmic frequencies of surrounding vehicles. (c) Inferred probabilistic driver space.**



**Figure 3: Relations between the estimated parameters and the relative speed.**

$$p(x, y, v) = \exp \left( - \left| \frac{x}{r_x} \right|^{\beta_x} - \left| \frac{y}{r_y} \right|^{\beta_y} \right),$$

where

$$\begin{cases} r_x = 0.0623v + 2.15, \\ r_y = 0.2526v^2 + 1.1650v + 3.55, \\ \beta_x = \frac{1+\text{sgn}(x)}{2} \cdot 4.776 + \frac{1-\text{sgn}(x)}{2} \cdot 4.298, \\ \beta_y = \frac{1+\text{sgn}(y)}{2} \cdot 3.413 + \frac{1-\text{sgn}(y)}{2} \cdot 2.815. \end{cases} \quad (6)$$

The values and relations of the parameters are of realistic implications.  $r_x$  and  $r_y$  refer to the lateral and longitudinal radius of driver space, respectively. The growth of them with  $v$  means larger driver space with the increasing relative speed between two vehicles, where the lateral radius grows at a constant rate but the longitudinal radius grows at an quadratic rate.  $\beta$ s refer to the increase rates of the discomfort across the boundaries of the driver space when a surrounding vehicle approaches the ego vehicle. Roughly speaking, the increase across the right boundary is slightly larger than the increase across the left boundary. They are larger than the increase across the front boundary, and the increase across the rear boundary is the smallest. Note that the left, right, front, and rear can be understood geographically only when the ego vehicle and its surrounding vehicles are moving in similar directions.

Summarising the visual and numerical results, we can make the following remarks. The discomfort of a vehicle caused by the intrusion of its driver space increases significantly faster across the lateral boundaries than across the longitudinal boundaries. This means that driver space has sharper lateral boundaries and longer longitudinal transitions extending outwards. Thereby, the traditional approaches based on (dis)comfort distance are only suitable for measuring the lateral but not the longitudinal size of driver space.

#### 4. CONCLUSIONS

This study proposes a probabilistic representation of driver space and a method for its empirical inference. The representation is a probability function of the proximity resistance of a vehicle to its surrounding vehicle. Its inference is the estimation of this probability function, which is achieved by maximising the joint probability of the presence of surrounding vehicles. We performed a series of experiments on a dataset of urban trajectories to demonstrate the methodology. Through the experiments, the relative speed of a vehicle to its surrounding vehicle is found to influence the size of its driver space both laterally and longitudinally. The results also find that the intrusion-caused discomfort increases much faster across the lateral boundaries than across the longitudinal boundaries of driver space. We therefore conclude that the traditional distance-based approach to measuring driver space are only suitable for the lateral measurement, but not for the longitudinal measurement.

Further work is expected to be done based on this study. The representation and measurement proposed in this study could be extended to the personal space for other entities such as bicycles or robotics. In the experiments in this study, the quality of the estimation is found to decrease as the relative speed increases. Such decrease could be related to the relative lack of samples, but remains to be explored. Research on how to obtain good estimates with sparse data is also needed. Besides, personal differences are ignored in this study due to the shortage of suitable data, but a verification of whether and to what extent personal differences exist is encouraged.

## ACKNOWLEDGMENT

This work is supported by the TU Delft AI Labs programme.

## REFERENCES

- Barmounakis, E., & Geroliminis, N. (2020). On the new era of urban traffic monitoring with massive drone data: The pneuma large-scale field experiment. *Transportation Research Part C: Emerging Technologies*, *111*, 50–71. doi: 10.1016/j.trc.2019.11.023
- Cheng, H., & Sester, M. (2018). Modeling mixed traffic in shared space using lstm with probability density mapping. In *2018 21st international conference on intelligent transportation systems (ITSC)* (pp. 3898–3904). doi: 10.1109/ITSC.2018.8569757
- Hayduk, L. A. (1978). Personal space: An evaluative and orienting overview. *Psychological bulletin*, *85*(1), 117–134. doi: 10.1037/0033-2909.85.1.117
- Hennessy, D. A. (2015). Personality predictors of driver space preference. In A. Columbus (Ed.), *Advances in psychology research* (Vol. 104, pp. 31–46). New York: Nova Science.
- Hennessy, D. A., Howard, S., & Carr, E. (2011). Driver space preference: Differences across age, gender and traffic conditions. In D. A. Hennessy (Ed.), *Traffic psychology: An international perspective* (pp. 233–250). New York: Nova Science Publishers.
- Leichtmann, B., & Nitsch, V. (2020). How much distance do humans keep toward robots? literature review, meta-analysis, and theoretical considerations on personal space in human-robot interaction. *Journal of Environmental Psychology*, *68*, 101386. doi: 10.1016/j.jenvp.2019.101386
- Marsh, P., & Collett, P. (1987). The car as a weapon. *ETC: A Review of General Semantics*, *44*(2), 146–151.
- Sommer, R. (1959). Studies in personal space. *Sociometry*, *22*(3), 247–260. doi: 10.2307/2785668
- Zhang, Q., Ge, Y., Qu, W., Hennessy, D. A., & Zhang, K. (2019). Effects of anger and collision history on driver space preference. *Transportation Research Part F: Traffic Psychology and Behaviour*, *63*, 108–117. doi: 10.1016/j.trf.2019.04.002